BioMedInformatics

CITESCORE 1.7

Article

Automated Classification of Collateral Circulation for Ischemic Stroke in Cone-Beam CT Images Using VGG11: A Deep Learning Approach

Nur Hasanah Ali, Abdul Rahim Abdullah, Norhashimah Mohd Saad, Ahmad Sobri Muda and Ervina Efzan Mhd Noor

MDPI

https://doi.org/10.3390/biomedinformatics4030091

BioMedInformatics

MDPI

Article

Automated Classification of Collateral Circulation for Ischemic Stroke in Cone-Beam CT Images Using VGG11: A Deep Learning Approach

Nur Hasanah Ali [1,*], Abdul Rahim Abdullah [2], Norhashimah Mohd Saad [3], Ahmad Sobri Muda [4] and Ervina Efzan Mhd Noor [1]

[1] Faculty of Engineering and Technology, Multimedia University, Jalan Ayer Keroh Lama, Bukit Beruang 75450, Melaka, Malaysia; ervina.noor@mmu.edu.my
[2] Faculty of Electrical Technology and Engineering, Universiti Teknikal Malaysia Melaka, Jalan Hang Tuah Jaya, Durian Tunggal 76100, Melaka, Malaysia; abdulr@utem.edu.my
[3] Faculty of Electronics and Computer Technology and Engineering, Universiti Teknikal Malaysia Melaka, Jalan Hang Tuah Jaya, Durian Tunggal 76100, Melaka, Malaysia; norhashimah@utem.edu.my
[4] Department of Imaging, Faculty of Medicine and Health Sciences, Universiti Putra Malaysia, Jalan Universiti 1, Serdang 43400, Selangor, Malaysia; asobri@upm.edu.my
* Correspondence: hasanah.ali@mmu.edu.my

Abstract: Background: Ischemic stroke poses significant challenges in diagnosis and treatment, necessitating efficient and accurate methods for assessing collateral circulation, a critical determinant of patient prognosis. Manual classification of collateral circulation in ischemic stroke using traditional imaging techniques is labor-intensive and prone to subjectivity. This study presented the automated classification of collateral circulation patterns in cone-beam CT (CBCT) images, utilizing the VGG11 architecture. Methods: The study utilized a dataset of CBCT images from ischemic stroke patients, accurately labeled with their respective collateral circulation status. To ensure uniformity and comparability, image normalization was executed during the preprocessing phase to standardize pixel values to a consistent scale or range. Then, the VGG11 model is trained using an augmented dataset and classifies collateral circulation patterns. Results: Performance evaluation of the proposed approach demonstrates promising results, with the model achieving an accuracy of 58.32%, a sensitivity of 75.50%, a specificity of 44.10%, a precision of 52.70%, and an F1 score of 62.10% in classifying collateral circulation patterns. Conclusions: This approach automates classification, potentially reducing diagnostic delays and improving patient outcomes. It also lays the groundwork for future research in using deep learning for better stroke diagnosis and management. This study is a significant advancement toward developing practical tools to assist doctors in making informed decisions for ischemic stroke patients.

Keywords: collateral circulation; CBCT image; VGG; classification

Citation: Ali, N.H.; Abdullah, A.R.; Saad, N.M.; Muda, A.S.; Noor, E.E.M. Automated Classification of Collateral Circulation for Ischemic Stroke in Cone-Beam CT Images Using VGG11: A Deep Learning Approach. *BioMedInformatics* **2024**, *4*, 1692–1702. https://doi.org/10.3390/biomedinformatics4030091

Academic Editor: James C. L. Chow

Received: 24 May 2024
Revised: 20 June 2024
Accepted: 28 June 2024
Published: 8 July 2024

1. Introduction

Ischemic stroke remains one of the leading causes of mortality and long-term disability worldwide, posing significant challenges to healthcare systems globally [1]. Rapid and accurate diagnosis of ischemic stroke is crucial for timely intervention and effective treatment, as delayed diagnosis can lead to irreversible neurological damage and worsened patient outcomes [2–5]. Collateral circulation typically occurs in ischemic stroke but not in hemorrhagic stroke. In ischemic stroke, when a blood vessel becomes blocked or narrowed, the body initiates a natural response known as angiogenesis [6,7]. Collateral circulation is the network of supplementary blood vessels that provide perfusion to the ischemic region, mitigating the impact of arterial occlusion and potentially salvaging threatened tissue [8–10], as shown in Figure 1.

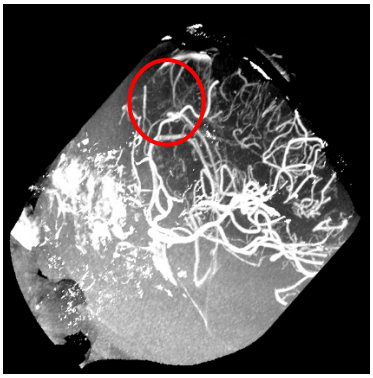

Figure 1. Visualization of collateral circulation.

Traditionally, the assessment of collateral circulation in ischemic stroke has relied on conventional imaging modalities such as computed tomography (CT) and magnetic resonance imaging (MRI), as stated by other researchers [11,12]. However, manual classification of collateral circulation patterns from these imaging modalities is labor-intensive, time-consuming, and subject to inter-observer variability [13]. Moreover, the complex and heterogeneous nature of collateral circulation patterns further complicates accurate classification using conventional methods. Numerous studies conducted by researchers have explored various scoring systems for characterizing collateral flow [14–16]. These systems aim to classify and assess the extent of collateral circulation, facilitating the evaluation of stroke severity and potential treatment outcomes. However, there is still a lack of consensus among experts regarding the most effective standardized scoring system for collateral circulation [17]. Each study on collateral circulation classification has its own unique set of characteristics and criteria. Table 1 provides a comparative analysis of the characteristics associated with poor, moderate, and good collateral circulation, offering insights into the distinctions and features of each classification category.

Table 1. Comparison between poor, moderate, and good collateral circulation.

Criteria	Poor	Moderate	Good
Assessment using the Miteff collateral method [14]	Only superficial MCA is reconstructed distal to the occlusion	Some of the MCA branches are reconstructed distal to the occlusion	Most of the MCA branches are reconstructed distal to the occlusion
Degree of vertebral venous expansion [15]	External vertebral vein $\leq$ 25%	External vertebral vein $\geq$ 25%	External vertebral vein $\geq$ 50%
Vascular reperfusion [18]	Minimal recanalization	Partial recanalization	Complete recanalization
Infarct growth [19]	More infarct growth with good pre-treatment.	Less infarct growth with good pre-treatment.	Did not show infarct growth with good pre-treatment.

Several medical imaging methods, including X-ray [20], cone-beam computed tomography (CBCT) [21,22], and magnetic resonance imaging (MRI) [23,24], offer detailed information concerning blood flow to different regions of the brain. Cone-beam computed tomography (CBCT) imaging offers a valuable tool for assessing collateral circulation due to its high spatial resolution [21,22,25,26] and ability to capture dynamic vascular changes [12,27], as shown in Figure 2. Collateral circulation patterns in CBCT images manifest as alterations in contrast enhancement, vessel caliber, and filling patterns, reflecting the compensatory blood flow routes established in response to arterial occlusion [27–29]. The identification and classification of these collateral circulation patterns are essential for understanding stroke pathophysiology and guiding treatment decisions. However, manual assessment of collateral circulation from CBCT images is challenging and prone to inter-observer variability [30]. Hence, the development of automated methods utilizing

deep learning techniques holds promise for providing rapid and objective evaluation of collateral circulation in ischemic stroke [31–33].

Figure 2. Example of CBCT images for collateral circulation.

In recent years, deep learning techniques have emerged as powerful tools for medical image analysis, offering the potential to automate and improve the accuracy of diagnostic tasks [34–37]. Convolutional neural networks (CNNs), in particular, have demonstrated remarkable performance in various medical imaging applications, including lesion detection, tumor segmentation, and disease classification [38,39]. Leveraging hierarchical features learned from large datasets, CNNs can extract discriminative features from medical images, enabling automated interpretation and diagnosis. VGG11 is particularly notable for its deep architecture and was among the early models to demonstrate the effectiveness of very deep networks in image classification tasks. Table 2 provides a review of the VGG11 technique.

Table 2. VGG11 Analysis Technique.

Author	Purpose	Imaging Modality	Result
Kaya et al. [40]	Skin Cancer	Skin cancer image	Accuracy—83%
Govindan et al. [41]	Sign Language	Hand gestures and voice	Accuracy—97.89%
Sri et al. [42]	Lung	X-ray	Accuracy—98.28%
Mao et al. [43]	Chicken Distress	Audio	Accuracy—95.07%
Rahi et al. [44]	Skin Cancer	Skin cancer image	Accuracy—85%

In this study, a novel deep-learning approach is proposed for the automated classification of collateral circulation patterns in cone-beam CT (CBCT) images of ischemic stroke patients. This study focuses on harnessing the capabilities of the VGG11 architecture, a deep CNN architecture known for its effectiveness in image classification tasks. By training VGG11 on a curated dataset of CBCT images, the development of a robust and accurate model capable of automatically classifying collateral circulation patterns. This method for assessing collateral circulation can significantly enhance clinical outcomes by providing rapid, accurate, and consistent evaluations, crucial for timely and personalized treatment decisions in stroke ischemic. Also, the method enables better risk stratification, optimizes resource allocation, and offers valuable prognostic information, leading to improved patient care and reduced complications.

2. Method

The proposed method implemented in this study is the VGG11 model, which is a variant of the VGG (Visual Geometry Group) architecture. The dataset was divided into 80% for training and 20% for testing, as shown in Figure 3, ensuring that the model is robustly trained and unbiasedly evaluated on unseen samples. The size and diversity of the training dataset significantly affect the performance of deep learning models. Larger datasets enhance model accuracy and feature learning, while diverse datasets improve generalization,

reduce bias, and increase robustness. Techniques such as data augmentation and transfer learning can further optimize dataset size and diversity. Thus, a well-structured and varied training dataset leads to better model performance, higher accuracy, and improved clinical outcomes in classifying collateral circulation in ischemic stroke.

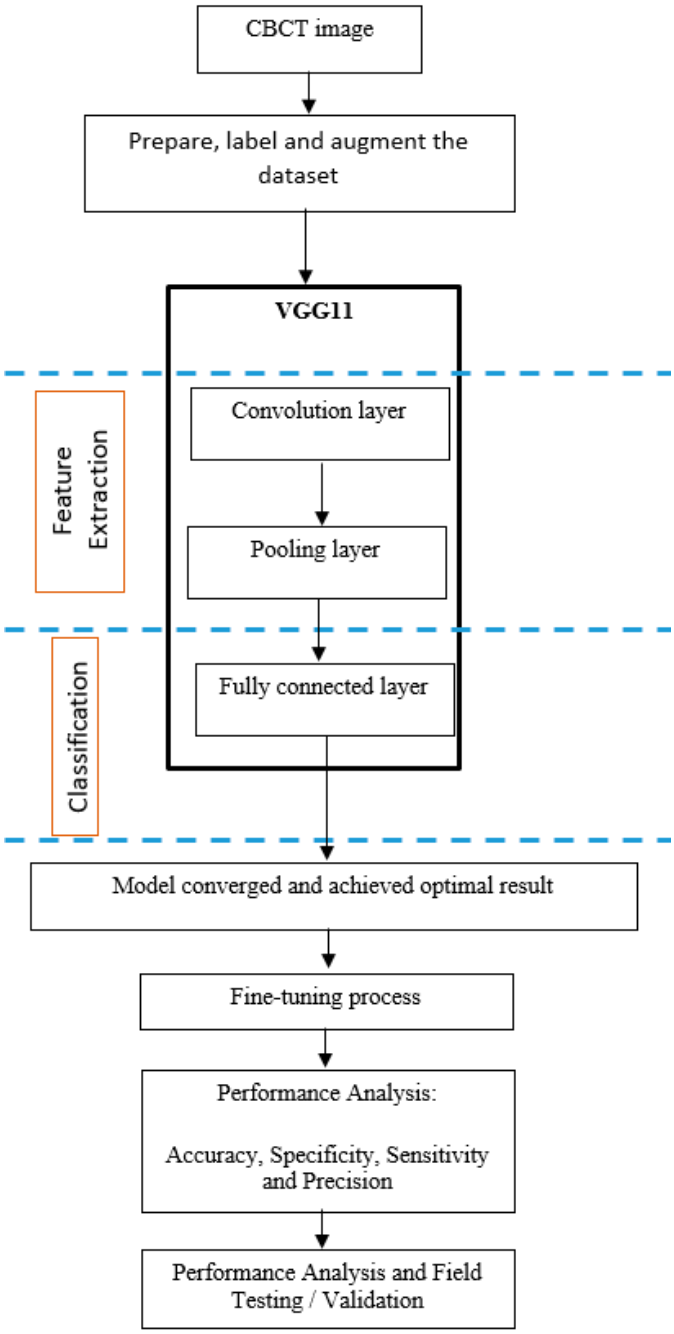

Figure 3. Research flow for VGG11 method.

In this study, VGG11 has been proposed to classify collateral circulation. The most significant advantage of using the VGG11 model is its simplicity and effectiveness in feature extraction, which leads to good accuracy in image classification tasks. VGG11 is a deep convolutional neural network architecture that was proposed by the Visual Geometry Group (VGG) based at the University of Oxford [38]. It is a variant of the VGG network architecture, originally introduced for image classification tasks. The VGG11 architecture is characterized by its deep structure and homogeneous design. The VGG11 model is composed of a sequence of convolutional layers, pooling layers, and fully connected layers.

The term "11" in VGG11 indicates the total count of layers in the network, encompassing both convolutional and fully connected layers [45].

The algorithm input data are an RGB image with a resolution of 256 by 256 pixels used for training and testing the deep learning models. Next, image pre-processing is implemented, where normalization and augmentation processes are involved. Image augmentation is a technique that involves applying various transformations to existing images in the dataset to generate additional training data.

Then, the model's architectures are selected and implemented. The architecture consists of seven convolutional layers, with each layer followed by a ReLU activation function. Furthermore, the model incorporates five 2×2 max pooling operations, progressively reducing the size of the feature maps by a factor of 2 at each pooling step [46]. It employs 3×3 kernels for all its convolutional layers, and Figure 4 provides details on the number of channels in each layer [45]. The first convolutional layer generates 64 channels, and as the network goes deeper, the number of channels doubles after each max pooling operation until it reaches 512. In the subsequent layers, the number of channels remains consistent [45].

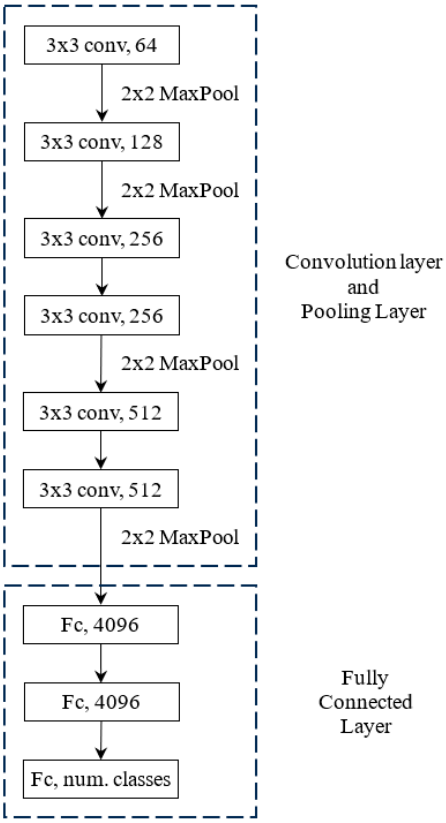

Figure 4. VGG11 architecture.

This method is also known for its simplicity and uniformity. By stacking multiple layers with small filters, it can learn hierarchical representations of increasing complexity. The deep structure of the network allows it to capture both low-level and high-level features in the input images, enabling it to achieve strong performance on image classification tasks.

The parameters of the network are optimized by employing a suitable loss function and an optimization algorithm like stochastic gradient descent (SGD), to train the model. Through backpropagation, the gradients of the loss with respect to the parameters are computed, and the parameter values are updated iteratively. The training process involves multiple epochs, with each epoch representing a full iteration over the entire training dataset [44]. Completing seven epochs allows the model to learn from training data and refine its parameters to enhance predictive capabilities. The primary training objective is

preventing overfitting, where the model becomes overly specialized and fails to generalize to new data [47]. The model's performance on the testing set is evaluated after each epoch, with accuracy serving as a crucial metric to ensure it doesn't overfit.

3. Results and Discussion

3.1. Training and Testing Stage

The sample image used for the VGG11 method is shown in Figure 5. Data sets of 3411 images were trained with the respective model, and the remaining 957 images were used to test the model's classification performance.

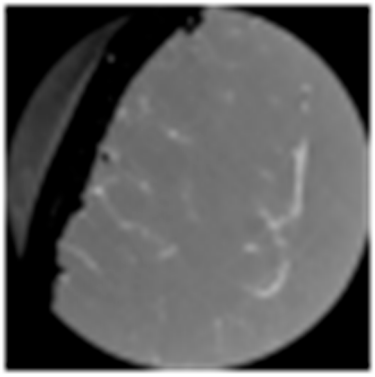

Figure 5. Sample CBCT image for VGG11 method.

Figure 6 illustrates the testing accuracy result of the proposed model, achieving the best accuracy of 58.32%. It visually represents the model's performance during testing, showcasing its accuracy across various evaluation metrics. The accuracy can be improved by considering a few aspects such as increasing the data size, and applying augmentation and regularization techniques. Furthermore, exploring more complex architectures or leveraging transfer learning from pre-trained models like VGG16, combined with meticulous preprocessing of input images, can further enhance accuracy by ensuring robust feature extraction and model stability.

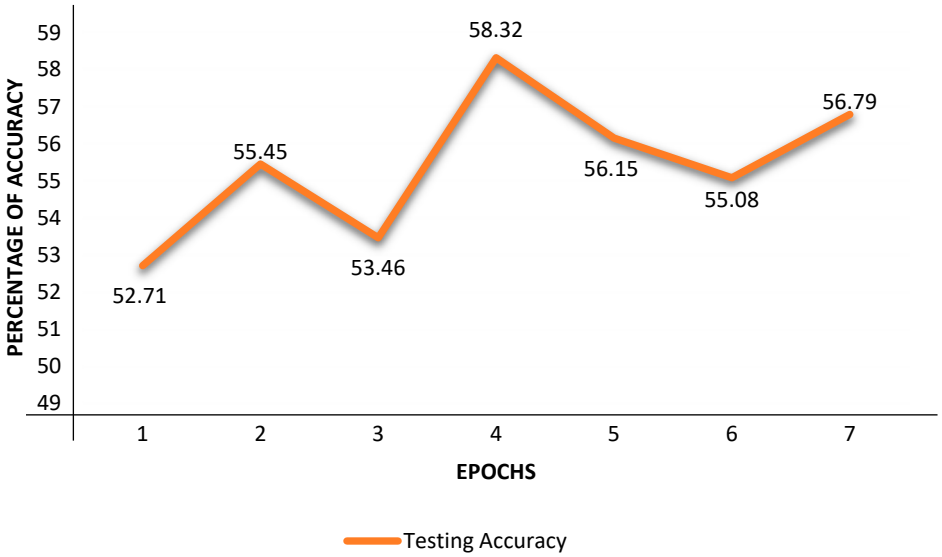

Figure 6. Testing accuracy graph for VGG11 method.

This result provides valuable insights for researchers and clinicians into the overall performance of the model and its ability to classify collateral circulation patterns accurately based on CBCT images. The achieved accuracy indicates that the model is learning meaningful patterns from the data and performing better than random chance. Furthermore, its

competitiveness with similar studies suggests comparable performance to existing methods, despite challenges such as noise, artifacts, and anatomical variability in the data. Therefore, while the accuracy may not be high, it represents a promising step forward in applying deep learning to collateral circulation classification in ischemic stroke. Further research and optimization efforts are necessary to improve accuracy and robustness, potentially through advanced architectures, larger datasets, and parameter fine-tuning.

Figure 7 shows the training and testing loss results for seven epochs. It shows the comparison between training and testing loss. The graph shows that the testing loss is greater than the training loss. This could be an indication that the model is overfitting. The model performs better on the training than the testing data set.

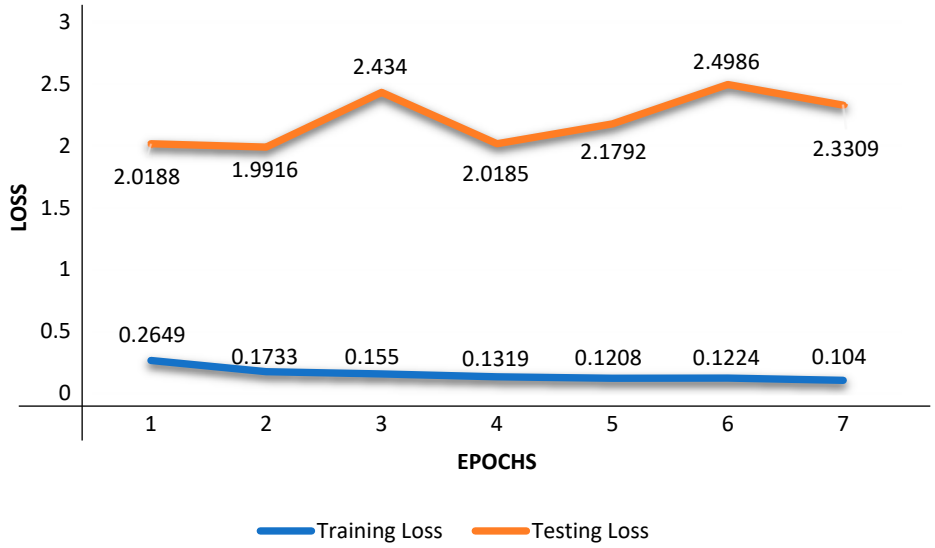

Figure 7. Training and testing loss comparison graph for VGG11 method.

3.2. Classification Stage

The confusion matrix depicted in Figure 8 provides a comprehensive evaluation of the classification performance of the VGG11 model on both the training and testing datasets. It allows for a detailed examination of the model's correct and incorrect classifications within each class.

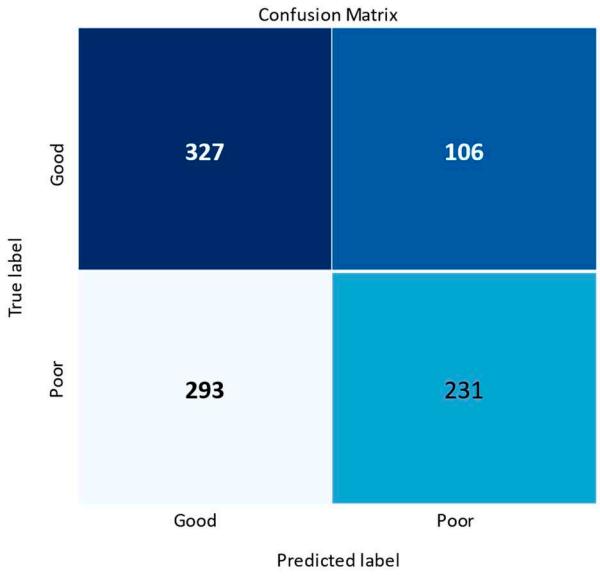

Figure 8. Confusion matrix for testing data for VGG11 method.

The confusion matrix reveals that the model demonstrates effective classification capabilities, as evidenced by the high number of correct predictions. Specifically, it correctly classifies 327 images as having good collateral circulation and 231 images as having poor collateral circulation. These accurate predictions indicate the model's ability to discern distinct patterns and features associated with different collateral circulation classes.

However, upon closer examination of the confusion matrix, it is evident that some samples are misclassified, leading to incorrect predictions. These misclassifications highlight the need for further investigation and improvement to enhance the model's accuracy. It becomes essential to identify the specific challenges and factors contributing to the misclassifications to provide the model with additional clarity and guidance for accurate classification.

By doing this, valuable insights into the model's performance and areas for refinement are identified. The matrix allows for a quantitative assessment of the classification results, providing a clear understanding of the strengths and limitations of the model in classifying collateral circulation based on CBCT images.

3.3. Performance Evaluation Stage

The performance of the model is evaluated through a series of experiments, yielding a comprehensive set of metric results. The effectiveness of the proposed system is meticulously assessed using a range of performance metrics discussed in detail within this section. These metrics provide valuable insights into the performance and accuracy of the models under evaluation, enabling a comprehensive analysis of their capabilities. For a comprehensive understanding of the models' performance, metrics such as accuracy, sensitivity, specificity, precision, and F1 score are calculated and analyzed. Based on the confusion matrix in Figure 8, the best accuracy of 58.32%, a sensitivity of 75.50%, a specificity of 44.10%, a precision of 52.70%, and an F1 score of 62.10% are obtained from the calculation below.

According to Equation (1), the accuracy calculation of the proposed model reveals an accuracy score of 58.30%. In this study, the model successfully predicted 327 images with good collateral circulation and 231 images with poor collateral circulation. This indicates that out of the total 957 images in the dataset, the model made correct predictions for 558 images, encompassing both categories of collateral circulation.

$$\begin{gathered} \text{Accuracy} = \frac{\text{True Positive} + \text{True Negative}}{\text{Total number of samples}} \\ \text{Accuracy} = \frac{327 + 231}{957} \\ \text{Accuracy} = 0.583 \end{gathered} \tag{1}$$

Equation (2) calculates the sensitivity of the proposed model, resulting in a sensitivity score of 75.50%. In this study, out of the total 433 images with good collateral circulation, the model successfully identified and classified 327 images as having good collateral circulation. This indicates that the model's ability to accurately detect and classify positive cases of good collateral circulation resulted in a high sensitivity score, demonstrating its effectiveness in identifying this specific category of collateral circulation patterns.

$$\begin{gathered} \text{Sensitivity} = \frac{\text{True Positive}}{\text{True Positive} + \text{False Negative}} \\ \text{Sensitivity} = \frac{327}{327 + 106} \\ \text{Sensitivity} = 0.755 \end{gathered} \tag{2}$$

Equation (3) calculated the specificity of the proposed model and determined that the specificity value is 44.10%. In this study, out of the total 524 images illustrating poor

collateral circulation, the model successfully identified and classified 231 images as having poor collateral circulation.

$$\begin{gathered} \text{Specificity} = \frac{\text{True Negative}}{\text{True Negative} + \text{False Positive}} \\ \text{Specificity} = \frac{231}{231 + 293} \\ \text{Specificity} = 0.441 \end{gathered} \tag{3}$$

Upon performing the precision calculation in Equation (4), it is determined that the precision value is 52.70%. In this study, out of all the positive predictions made by the model, which include both true positive and false positive predictions, 52.70% of them correspond to true positive predictions, meaning they correctly identify instances of good collateral circulation. This precision score suggests that while the model demonstrates a reasonable level of accuracy in identifying positive cases, there is still room for improvement in terms of reducing the number of false positive predictions. Further optimization and fine-tuning of the model may enhance its precision and overall performance in accurately identifying and classifying cases of good collateral circulation.

$$\begin{gathered} \text{Precision} = \frac{\text{True Positive}}{\text{True Positive} + \text{False Positive}} \\ \text{Precision} = \frac{327}{327 + 293} \\ \text{Precision} = 0.527 \end{gathered} \tag{4}$$

Upon calculating the F1 score in Equation (5), it has been determined that the F1 score value is 62.10%. In this study, the F1 score reflects how precise the model is in identifying cases of good collateral circulation. Achieving a higher F1 score would require enhancing both precision and sensitivity, thereby improving the model's ability to accurately classify cases of good collateral circulation. This could be accomplished through further refinement and optimization of the model, considering factors such as feature selection, hyperparameter tuning, and data augmentation techniques.

$$\begin{gathered} \text{F1 score} = \frac{2 \times \text{Precision} \times \text{Sensitivity}}{\text{Precision} + \text{Sensitivity}} \\ \text{F1 score} = \frac{2 \times 0.527 \times 0.755}{0.527 + 0.755} \\ \text{F1 score} = 0.621 \end{gathered} \tag{5}$$

4. Conclusions

This study demonstrates the potential of deep learning using the VGG11 method, to automate the classification of collateral circulation patterns in ischemic stroke using CBCT imaging. The study achieved a notable accuracy of 58.32% in accurately classifying collateral circulation patterns, demonstrating the potential of deep learning techniques, particularly with the VGG11 architecture, in this domain. Although the achieved accuracy is competitive with other studies, further advancements are needed to improve classification accuracy and robustness for real-world clinical applications. This research contributes to the ongoing efforts to utilize deep learning for more accurate and efficient stroke diagnosis and optimizing treatment strategies.

Author Contributions: Conceptualization, N.H.A.; methodology, N.H.A.; validation, A.S.M.; formal analysis, N.H.A.; data curation, A.S.M.; writing—original draft preparation, N.H.A.; writing—review and editing, E.E.M.N.; supervision, A.R.A. and N.M.S.; funding acquisition, N.H.A. All authors have read and agreed to the published version of the manuscript.

Funding: The APC was funded by Multimedia University (MMU/RMC/PC/2024/151807).

Institutional Review Board Statement: Not applied.

Data Availability Statement: The datasets presented in this article are not readily available due to patient confidentiality. Requests to access the datasets should be directed to the corresponding author.

Conflicts of Interest: The authors declare no conflict of interest.

References

1. Basiron, H.; Azmi, M.A.; Latif, M.J.A.; Kamaruddin, A.I.; Zaidi, A.I.M.; Badrulzaman, W.M.F.W. Development of Speech Therapy Mobile Application for Speech Disorder Post-Stroke Patients. In Proceedings of the 2021 IEEE 11th International Conference on System Engineering and Technology (ICSET), Shah Alam, Malaysia, 6 November 2021; pp. 130–133.
2. Lyden, S.; Wold, J. Acute Treatment of Ischemic Stroke. *Neurol. Clin.* **2022**, *40*, 17–32. [CrossRef] [PubMed]
3. Bandzouzi, P.E.G.S.; Mpandzou, G.A.; Diatewa, J.E.; M'foutou, P.M.; Motoula-Latou, D.H.; Koubemba, C.G.; Ossou-Nguiet, P.M.; Moukassa, D. Stroke and HIV: Correlation between Viral Load and Type of Stroke. *Neurosci. Med.* **2021**, *12*, 163–167. [CrossRef]
4. Emon, M.U.; Keya, M.S.; Meghla, T.I.; Rahman, M.; Al Mamun, M.S.; Kaiser, M.S. Performance Analysis of Machine Learning Approaches in Stroke Prediction. In Proceedings of the 2020 4th International Conference on Electronics, Communication and Aero-space Technology (ICECA), Coimbatore, India, 5–7 November 2020; pp. 1464–1469. [CrossRef]
5. Agbetou, M.; Sowanou, A.; Goudjinou, G.; Adjien, C.; Houinato, D.; donné Gnonlonfoun, D. Etiologies of Ischemic Stroke in Sub-Saharan Africa, Case of Benin. *Neurosci. Med.* **2020**, *11*, 100–107. [CrossRef]
6. Zhu, H.; Zhang, Y.; Zhong, Y.; Ye, Y.; Hu, X.; Gu, L.; Xiong, X. Inflammation-Mediated Angiogenesis in Ischemic Stroke. *Front. Cell. Neurosci.* **2021**, *15*, 652647. [CrossRef] [PubMed]
7. Kui, L.; Li, Z.; Wang, G.; Li, X.; Zhao, F.; Jiao, Y. CircPDS5B Reduction Improves Angiogenesis Following Ischemic Stroke by Regulating MicroRNA-223-3p/NOTCH2 Axis. *Neurol. Genet.* **2023**, *9*, e200074. [CrossRef] [PubMed]
8. Agarwal, A.; Sharma, A.; Vishnu, V.; Srivastava, M.P. Collateral Circulation—Evolving from Time Window to Tissue Window. *Ann. Indian Acad. Neurol.* **2022**, *26*, 10–16. [CrossRef]
9. Vasquez, H.E.; Murlimanju, B.V.; Shrivastava, A.; Durango-Espinosa, Y.A.; Joaquim, A.F.; Garcia-Ballestas, E.; Moscote-Salazar, L.R.; Agrawal, A. Intracranial collateral circulation and its role in neurovascular pathology. *Egypt. J. Neurosurg.* **2021**, *36*, 2. [CrossRef]
10. Verdolotti, T.; Pilato, F.; Cottonaro, S.; Monelli, E.; Giordano, C.; Guadalupi, P.; Benenati, M.; Ramaglia, A.; Costantini, A.M.; Alexandre, A.; et al. Colorviz, a new and rapid tool for assessing collateral circulation during stroke. *Brain Sci.* **2020**, *10*, 882. [CrossRef]
11. Shokri, A.; Eskandarloo, A.; Norouzi, M.; Poorolajal, J.; Majidi, G.; Aliyaly, A. Diagnostic accuracy of cone-beam computed tomography scans with high- and low-resolution modes for the detection of root perforations. *Imaging Sci. Dent.* **2018**, *48*, 11–19. [CrossRef]
12. Iqbal, S. A comprehensive study of the anatomical variations of the circle of Willis in adult human brains. *J. Clin. Diagn. Res.* **2013**, *7*, 2423–2427. [CrossRef]
13. Malhotra, K.; Liebeskind, D.S. Collaterals in ischemic stroke. *Brain Hemorrhages* **2020**, *1*, 6–12. [CrossRef]
14. Liu, L.; Ding, J.; Leng, X.; Pu, Y.; Huang, L.-A.; Xu, A.; Wong, K.S.L.; Wang, X.; Wang, Y. Guidelines for evaluation and management of cerebral collateral circulation in ischaemic stroke 2017. *Stroke Vasc. Neurol.* **2018**, *3*, 117–130. [CrossRef]
15. Wang, Z.; Ding, J.; Bai, C.; Ding, Y.; Ji, X.; Meng, R. Clinical Classification and Collateral Circulation in Chronic Cerebrospinal Venous Insufficiency. *Front. Neurol.* **2020**, *11*, 913. [CrossRef] [PubMed]
16. Bang, O.Y.; Saver, J.L.; Kim, S.J.; Kim, G.-M.; Chung, C.-S.; Ovbiagele, B.; Lee, K.H.; Liebeskind, D.S.; CLA-Samsung Stroke Collaborators. Collateral flow averts hemorrhagic transformation after endovascular therapy for acute ischemic stroke. *Stroke* **2011**, *42*, 2235–2239. [CrossRef]
17. Potter, C.A.; Vagal, A.S.; Goyal, M.; Nunez, D.B.; Leslie-Mazwi, T.M.; Lev, M.H. CT for treatment selection in acute ischemic stroke: A code stroke primer. *Radiographics* **2019**, *39*, 1717–1738. [CrossRef] [PubMed]
18. Bang, O.Y.; Saver, J.L.; Kim, S.J.; Kim, G.-M.; Chung, C.-S.; Ovbiagele, B.; Lee, K.H.; Liebeskind, D.S. Collateral flow predicts response to endovascular therapy for acute ischemic stroke. *Stroke* **2011**, *42*, 693–699. [CrossRef]
19. Bang, O.Y.; Saver, J.L.; Buck, B.H.; Alger, J.R.; Starkman, S.; Ovbiagele, B.; Kim, D.; Jahan, R.; Duckwiler, G.R.; Yoon, S.R.; et al. Impact of collateral flow on tissue fate in acute ischaemic stroke. *J. Neurol. Neurosurg. Psychiatry* **2008**, *79*, 625–629. [CrossRef]
20. Nicholson, P.; Cancelliere, N.M.; Bracken, J.; Hummel, E.; van Nijnatten, F.; Withagen, P.; van de Haar, P.; Hallacoglu, B.; van Vlimmeren, M.; Agid, R.; et al. Novel flat-panel cone-beam CT compared to multi-detector CT for assessment of acute ischemic stroke: A prospective study. *Eur. J. Radiol.* **2021**, *138*, 109645. [CrossRef]
21. Yang, T.-W.; Lin, Y.-Y.; Hsu, S.-C.; Chu, K.C.-W.; Hsiao, C.-W.; Hsu, C.-W.; Bai, C.-H.; Chang, C.-K.; Hsu, Y.-P. Diagnostic performance of cone-beam computed tomography for scaphoid fractures: A systematic review and diagnostic meta-analysis. *Sci. Rep.* **2021**, *11*, 2587. [CrossRef]
22. Aziz, A.A.; Izhar, L.I.; Asirvadam, V.S.; Tang, T.B.; Ajam, A.; Omar, Z.; Muda, S. Detection of Collaterals from Cone-Beam CT Images in Stroke. *Sensors* **2021**, *21*, 8099. [CrossRef]
23. Phipps, M.S.; Cronin, C.A. Management of acute ischemic stroke. *BMJ* **2020**, *368*, l6983. [CrossRef] [PubMed]
24. Saad, N.M.; Abdullah, A.R.; Syafeeza, A.R.; Noor, N.S.M.; Ali, N.H.; Muda, A.S. Automated Classification of Stroke Lesion Using Bagged Tree Classifier. *IOP Conf. Ser. Mater. Sci. Eng.* **2020**, *884*, 012078. [CrossRef]
25. Lata, S.; Mohanty, S.K.; Vinay, S.; Das, A.C.; Das, S.; Choudhury, P. Is Cone Beam Computed Tomography (CBCT) a Potential Imaging Tool in ENT Practice?: A Cross-Sectional Survey Among ENT Surgeons in the State of Odisha, India. *Indian J. Otolaryngol. Head Neck Surg.* **2018**, *70*, 130–136. [CrossRef] [PubMed]
26. Kabaliuk, N.; Nejati, A.; Loch, C.; Schwass, D.; Cater, J.E.; Jermy, M.C. Strategies for Segmenting the Upper Airway in Cone-Beam Computed Tomography (CBCT) Data. *Open J. Med. Imaging* **2017**, *07*, 196–219. [CrossRef]

27. Jamaiyar, A.; Juguilon, C.; Dong, F.; Cumpston, D.; Enrick, M.; Chilian, W.M.; Yin, L. Cardioprotection during ischemia by coronary collateral growth. *Am. J. Physiol.-Heart Circ. Physiol.* **2019**, *316*, H1–H9. [CrossRef] [PubMed]
28. Mayer, L.; Grams, A.; Freyschlag, C.F.; Gummerer, M.; Knoflach, M. Management and prognosis of acute extracranial internal carotid artery occlusion. *Ann. Transl. Med.* **2020**, *8*, 1268. [CrossRef]
29. Piedade, G.S.; Schirmer, C.M.; Goren, O.; Zhang, H.; Aghajanian, A.; Faber, J.E.; Griessenauer, C.J. Cerebral Collateral Circulation: A Review in the Context of Ischemic Stroke and Mechanical Thrombectomy. *World Neurosurg.* **2019**, *122*, 33–42. [CrossRef] [PubMed]
30. Tetteh, G.; Navarro, F.; Meier, R.; Kaesmacher, J.; Paetzold, J.C.; Kirschke, J.S.; Zimmer, C.; Wiest, R.; Menze, B.H. A deep learning approach to predict collateral flow in stroke patients using radiomic features from perfusion images. *Front. Neurol.* **2023**, *14*, 1039693. [CrossRef]
31. Kersten-Oertel, M.; Alamer, A.; Fonov, V.; Lo, B.W.Y.; Tampieri, D.; Collins, D.L. Towards a computed collateral circulation score in ischemic stroke. *arXiv* **2020**, arXiv:2001.07169.
32. Aktar, M.; Tampieri, D.; Rivaz, H.; Kersten-Oertel, M.; Xiao, Y. Automatic collateral circulation scoring in ischemic stroke using 4D CT angiography with low-rank and sparse matrix decomposition. *Int. J. Comput. Assist. Radiol. Surg.* **2020**, *15*, 1501–1511. [CrossRef]
33. Ali, N.H.; Abdullah, A.R.; Saad, N.M.; Muda, A.S. Brain cone beam computed tomography image analysis using ResNet50 for collateral circulation classification. *Int. J. Electr. Comput. Eng.* **2023**, *13*, 5843–5852. [CrossRef]
34. Biratu, E.S.; Schwenker, F.; Debelee, T.G.; Kebede, S.R.; Negera, W.G.; Molla, H.T. Enhanced Region Growing for Brain Tumor MR Image Segmentation. *J. Imaging* **2021**, *7*, 22. [CrossRef]
35. Zhi, S.; Kachelrieb, M.; Pan, F.; Mou, X. CycN-Net: A Convolutional Neural Network Specialized for 4D CBCT Images Refinement. *IEEE Trans. Med. Imaging* **2021**, *40*, 3054–3064. [CrossRef]
36. Wan, Z.; Liu, C.; Zhang, M.; Fu, J.; Wang, B.; Cheng, S.; Ma, L.; Quilodrán-Casas, C.; Arcucci, R. Med-UniC: Unifying Cross-Lingual Medical Vision-Language Pre-Training by Diminishing Bias. *arXiv* **2023**, arXiv:2305.19894.
37. Liu, C.; Cheng, S.; Chen, C.; Qiao, M.; Zhang, W.; Shah, A.; Bai, W.; Arcucci, R. M-FLAG: Medical Vision-Language Pre-training with Frozen Language Models and Latent Space Geometry Optimization. In *Lecture Notes in Computer Science (including Subseries Lecture Notes in Artificial Intelligence and Lecture Notes in Bioinformatics)*; Springer: Cham, Switzerland, 2023; Volume 14220, pp. 637–647.
38. Alom, M.Z.; Taha, T.M.; Yakopcic, C.; Westberg, S.; Sidike, P.; Nasrin, M.S.; Hasan, M.; Van Essen, B.C.; Awwal, A.A.; Asari, V.K. A state-of-the-art survey on deep learning theory and architectures. *Electronics* **2019**, *8*, 292. [CrossRef]
39. Talo, M.; Yildirim, O.; Baloglu, U.B.; Aydin, G.; Acharya, U.R. Convolutional neural networks for multi-class brain disease detection using MRI images. *Comput. Med. Imaging Graph.* **2019**, *78*, 101673. [CrossRef] [PubMed]
40. Kaya, V.; Akgül, I. Classification of skin cancer using VGGNet model structures. *Gümüşhane Üniversitesi Fen Bilimleri Dergisi* **2022**, *13*, 190–198. [CrossRef]
41. Govindan, A.P.; Kumarappan, A. A Reversible Convolutional Neural Network Model for Sign Language Recognition. *Int. J. Intell. Eng. Syst.* **2022**, *15*, 163–174.
42. Sri, S.V.; Kavya, S. Lung Segmentation Using Deep Learning. *Asian J. Appl. Sci. Technol.* **2021**, *05*, 10–19. [CrossRef]
43. Mao, A.; Giraudet, C.S.E.; Liu, K.; Nolasco, I.D.A.; Xie, Z.; Xie, Z.; Gao, Y.; Theobald, J.; Bhatta, D.; Stewart, R.; et al. Automated identification of chicken distress vocalizations using deep learning models. *J. R. Soc. Interface* **2022**, *19*, 20210921. [CrossRef]
44. Rahi, M.I.; Khan, F.T.; Mahtab, M.T.; Ullah, A.K.M.A.; Alam, G.R.; Alam, A. Detection Of Skin Cancer Using Deep Neural Networks. In Proceedings of the 2019 IEEE Asia-Pacific Conference on Computer Science and Data Engineering (CSDE), Melbourne, VIC, Australia, 9–11 December 2019.
45. Iglovikov, V.; Shvets, A. TernausNet: U-Net with VGG11 Encoder Pre-Trained on ImageNet for Image Segmentation. *arXiv* **2018**, arXiv:1801.05746.
46. Tammina, S. Transfer learning using VGG-16 with Deep Convolutional Neural Network for Classifying Images. *Int. J. Sci. Res. Publ.* **2019**, *9*, 143–150. [CrossRef]
47. Sanjar, K.; Rehman, A.; Paul, A.; JeongHong, K. Weight dropout for preventing neural networks from overfitting. In Proceedings of the 2020 8th International Conference on Orange Technology (ICOT 2020), Daegu, Republic of Korea, 18–21 December 2020; pp. 3–6.